The optimum color operator for recovering low frequencies

Sina Esmaeili and Gary F. Margrave

ABSTRACT

Most Seismic data processing algorithms try to shape seismic data into a white spectrum during deconvolution procedure. In reality most natural occurring reflectivity sequences have colored spectra instead of white spectra. Studying the actual earth reflectivity and its spectra's shape are showing that the effect of colored spectra is more significant in frequencies below than 50Hz.

We study the spectral property of seismic data, and by using the well reflectivity, we introduce a new technique to shape the white spectrum of deconvolved data into the colored spectrum of reflectivity. This leads to better recovery of the low frequency component and hence better inversion.

INTRODUCTION

In processing data conventional deconvolution tries to remove the wavelet effect from seismic data and shape the spectra to a white one (Gary Margrave, 2002). Walden and Hosken (1985) showed that the most reflectivities from wells sourced all over the world do not have white spectra. Therefore any result comes from conventional deconvolution will not estimate the reflectivity properly. On the other hand, the assumptions which are used in the deconvolution algorithm cannot satisfy the color effects. To correct the color properties of real reflectivity for estimated data we need to define an operator which can recover the lost data.

This can be done by designing a suitable color operator. A color operator is a convolutional minimum phase operator which can be applied to the output of any deconvolved data to correct for a non-white reflectivity. The operator must be minimum phase because the deconvolution operator that whitened the spectrum was minimum phase. The desired color operator can be designed in many different ways. The main concept is to use real reflectivity which is available in well location and its Fourier transformation in frequency domain. Once the amplitude spectrum of real reflectivity is calculated, the amplitude spectrum of the color operator can be derived by curve fitting technique. We investigate several models for spectral color like the sigmoidal function or arctan function. The color operator should be applied to the seismic data right after deconvolution process to shape the whitened result from deconvolution into the reflectivity's colored spectrum. Once this is done the trace is said to be colored and further processing including inversion can proceed.

A well from Alberta (Husky Hussar 12-27) is used in this study and 15Hz minimum phase wavelet will was used. The synthetic seismic data were created by both "*Seismo*" and "*Syngram*" algorithms from the CREWES toolbox. The seismo algorithm creates a 1D normal incidence seismogram while Syngram creates a P-P and P-S AVO gather. At the end of this paper for further comparison the impedance inversions are shown

METHOD

A frequency domain deconvolution is based on four assumptions: (1) wavelet should be minimum phase; (2) wavelet spectrum should be smooth; (3) wavelet should be stationary; and (4) reflectivity should be random so its spectrum becomes white. However, as was mentioned, the real earth reflectivity has a colored spectrum and if we want to estimate this type of reflectivity via frequency domain deconvolution algorithm, it will be affected by white spectrum assumption (Figure 1).

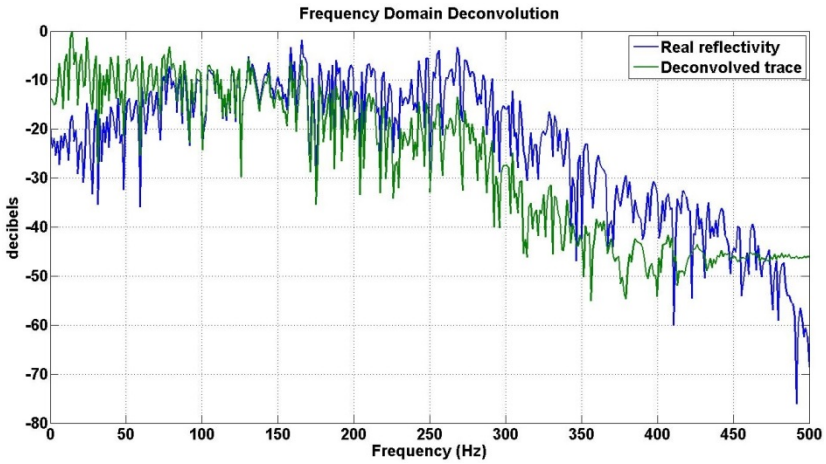

FIG.1. The effect of frequency domain deconvolution with white spectrum assumption on deconvolved data. The reflectivity color refers to the spectral roll-off below 75 Hz. The roll off above 250 Hz is artificial and is due to an anti-alias filter.

From examination of Figure 1 the deconvolved data below than 75Hz follow a white spectrum and depart significantly from the colored spectrum of the reflectivity. Note that we are not interested in the spectral shape of the reflectivity for frequencies higher than 250Hz since these frequencies are shaped by an anti-alias filter. The real reflectivity from well has very high sample rate which in time is roughly around every 0.1 milliseconds. However the sample rate of seismogram is usually around one or two milliseconds and therefore the well log data must be downsampled. Whenever a signal goes from more samples to fewer samples, an anti-alias filter is required. Thus the creation of a synthetic seismogram from well log requires an anti-alias filter. A typical anti-alias filter has an amplitude spectrum which begins to roll off at 50% to 60% of Nyquist frequency and reaches very large attenuation at Nyquist frequency. That is why the amplitude spectrum of reflectivity starts to decay after 250Hz in Figure 1. For example the well reflectivity of two different wells from Alberta with three different sample rates, 0.002; 0.001 and 0.0005, in time and frequency domain are shown in Figure 2. Using higher sample rates shifts the anti-alias filter effect to higher frequencies, revealing an essentially flat spectrum. The spectral color that we are concerned with is the decreasing spectrum as frequency drops below about 75 Hz. It is this effect that we wish to model.

In frequency domain deconvolution, correcting the white spectrum assumption can be done with an operator that, if applied to the deconvolved data, corrects the spectral shape at low frequencies. This operator should depend only on the observed spectral shape of the reflectivity, and be minimum phase. Three different algorithms to derive the color operator will be discussed and compared in this paper. The color operator in frequency domain includes both amplitude and phase spectrum. Based on the amplitude spectral shape of earth reflectivity (figure 1), the amplitude spectrum of color operator can be derived by fitting any appropriate function to the amplitude spectrum of reflectivity (figure 3). Once the amplitude spectrum of color operator is calculated its phase can be calculated by Hilbert transform of the logarithm of the amplitude spectrum. We will design a color operator that has a very smooth spectrum in the hope that it will have wide applicability.

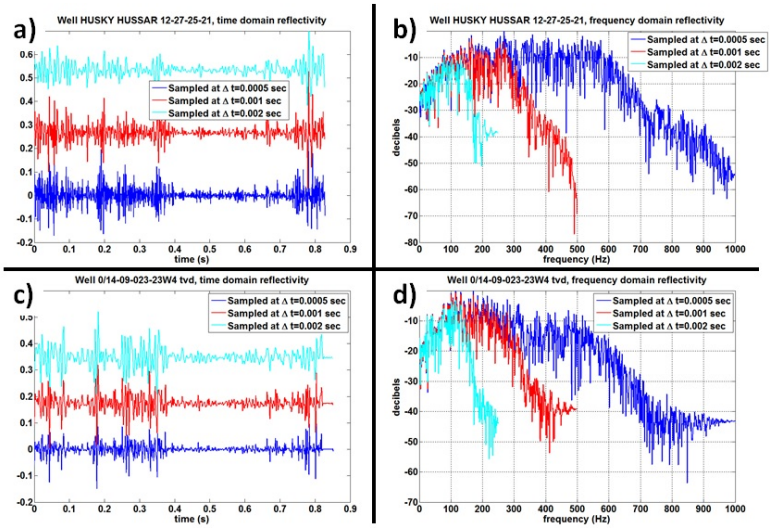

FIG.2. A comparison of well log reflectivity for two different Alberta wells in the time and frequency domains. a) and b) are well 1227 (Hussar) while c) and d) are well 1409 (Blackfoot). The time domain views are a) and c) while b) and d) are the frequency domain. The frequency domain views show clearly the effect of the anti-alias filter which begins its roll off at ½ of the Nyquist frequency. The low frequency roll off is essentially independent of sample rate and is similar for both wells. This low frequency roll off is what is modelled by our color operators.

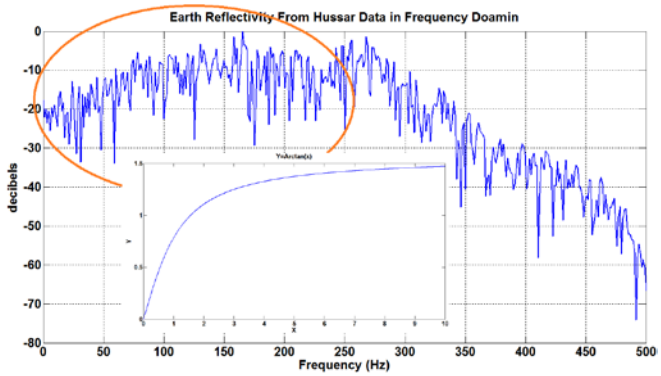

FIG.3. Earth reflectivity from Hussar data in frequency domain and Arctan(x) have a similar shape.

One possible function to fit on reflectivity's amplitude spectrum based on figure 3 is the arctan function. Mathematically, for fitting arctan function into the reflectivity function we can write

$$a + b\arctan(f) = R(f), \tag{1}$$

where a and b are constants and should be determined and $R(f)$ is the amplitude spectrum of reflectivity function in term of frequency. In matrix representation equation (1) can be written as

$$[1 \quad \arctan(f)]_{n\times 2}\begin{bmatrix} a \\ b \end{bmatrix}_{2\times 1} = A\begin{bmatrix} a \\ b \end{bmatrix} = R_{n\times 1}, \tag{2}$$

where 1 in the left hand side is n-by-1 matrix and n is the length of frequency (f). To find a and b in equation (2), both sides should be multiply by inverse of $[1 \quad \arctan(f)]_{n\times 2}$ from the left

$$\begin{bmatrix} a \\ b \end{bmatrix}_{2\times 1} = \left(A^T A\right)^{-1} A^T R. \tag{3}$$

By finding a and b the appropriate Arctan function related to the well reflectivity can be determined. We call this color operator the arctan color operator. For example for the well 12-27 from Hussar data a and b become 0.1623 and 0.9854 respectively. In the figure 4 the color operator and its amplitude spectrum in frequency domain are shown.

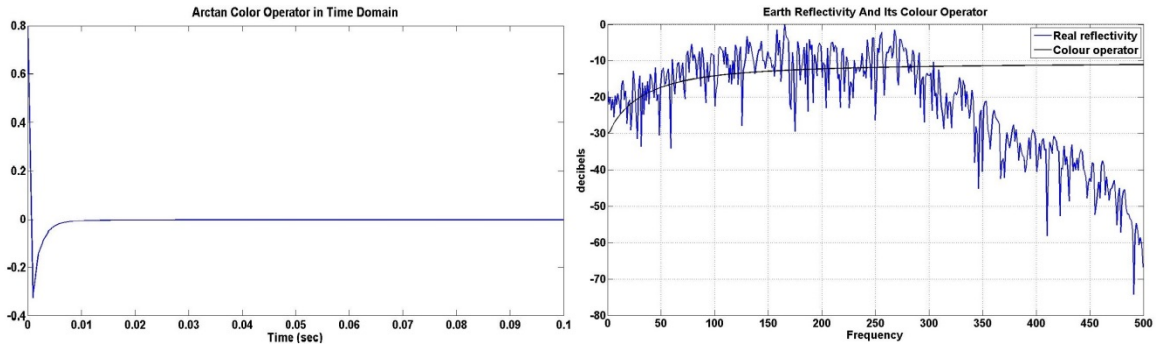

FIG.4. The Arctan color operator (left) and its amplitude spectrum in frequency domain (right).

As it is clear from this figure if the color operator applied to the deconvolved data (data in figure 1) it can shape the spectrum but there are possible problems at the very low frequencies. Further results will be discussed in the next section.

Examination of the frequencies below than 10Hz shows this part has a locally flattened shape which is not well modelled by the arctan function. Another possible model for color operator's amplitude spectrum including the horizontal part at low frequencies is fitting a sigmoidal function into the earth reflectivity amplitude spectrum. The mathematical form of the sigmoid function is

$$S(f)=\frac{\text{a+bs}}{\sqrt{1+\text{s}^2}};s=\frac{f-f_0}{f_0}, \tag{4}$$

where again *a* and *b* are the constants which should be determined by a similar procedure as used with the arctan function. The same calculations give us the other color operator with *a=-17.3914* and *b=7.6129*. This color operator and its amplitude spectrum are illustrated in figure 4.

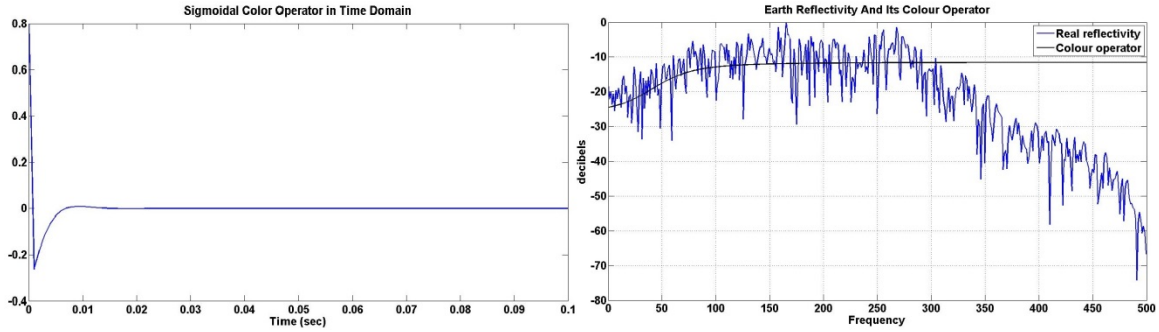

FIG.5. The Sigmoidal color operator (left) and its amplitude spectrum in frequency domain (right).

The third approach for color operator we study in this paper is significantly different from the first two. Suppose there is zero-offset receiver very near the well. Since all the information such as velocity, density and depth are available at the well location, we will form the ratio of the amplitude spectrum of the reflectivity divided by that of the deconvolved trace. After smoothing this ratio we will use it to construct a third minimum-phase color operator. Mathematically, this means

$$\alpha=\left[\frac{R(f)}{Tr(f)}\right]\bullet b(f), \tag{5}$$

where *R(f)* and *Tr(f)* are amplitude spectrum of well reflectivity and deconvolved data and $b(f)$ is a suitable convolutional smoother. The function *α(f)* with be a smoothed representation of the color operator amplitude spectrum. Its phase can be calculated by Hilbert transform. Once the color operator is calculated it can be applied by convolution as in the first two cases.

SEISMIC DATA PROCESSING

In September 2011, CREWES initiated a seismic experiment with the goal to push the low-frequency content of seismic data as low as possible. This project was located near Hussar, Alberta, which is about 100km east of Calgary, Alberta. The line was 4.5km long and it includes three wells 12-27, 14-27 and 14-35. In this paper two different types of synthetic data will be studied for the well 12-27. A zero-offset synthetic seismogram at the well location was created by *seismo* in CREWES Matlab toolbox and CMP gathers created by *Syngram* with the same well.

Zero-offset data processing

The zero-offset synthetic data in this paper are created by convolution of 15Hz minimum phase wavelet and reflectivity from well 12-27 data (Figure 6).

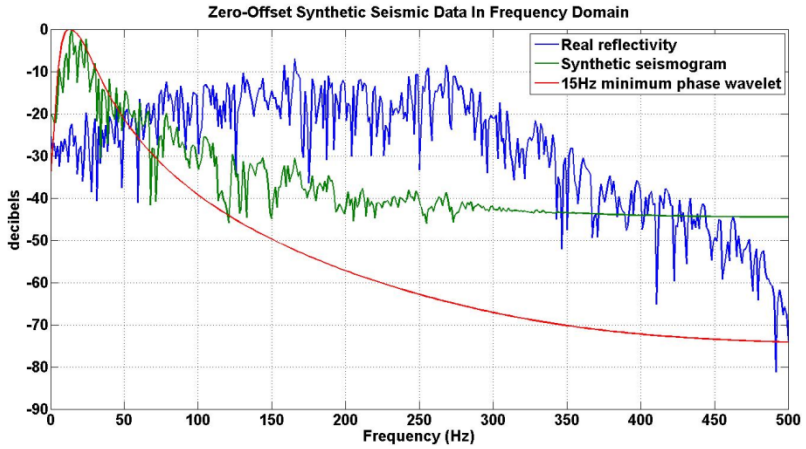

FIG.6. The amplitude spectrum of zero-offset synthetic data created by convolution of 15Hz minimum phase wavelet with reflectivity of well 12-27. Notice that the spectrum of the seismogram does not have the same shape as the wavelet. This is caused by the reflectivity color.

It is possible to show that the deconvolution results are directly dependent on the type of spectral smoother chosen (Esmaeili and Margrave, 2014). Their results demonstrate that the deconvolution algorithm with constant Gaussian smoother has better results than the deconvolution with frequency dependent Gaussian smoother or boxcar smoother. Based on these results, the zero-offset synthetic seismic trace in figure 6 can be deconvolved with the deconvolution algorithm with constant Gaussian smoother. The result is shown in figure 7.

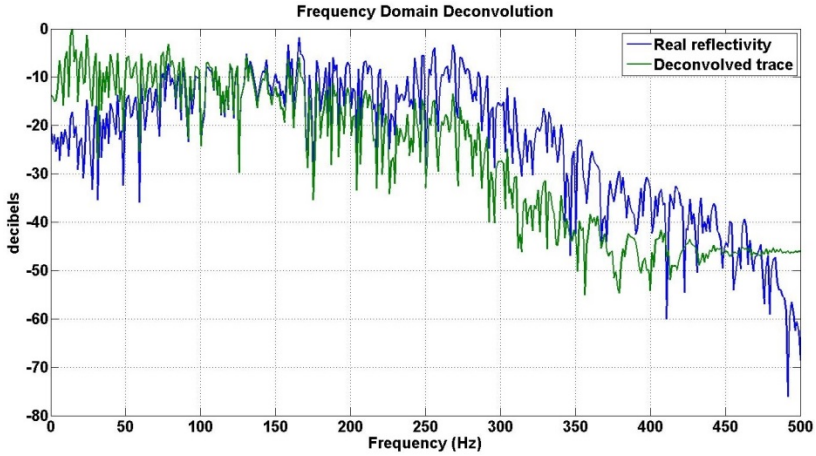

FIG.7. Comparing zero-offset synthetic seismic trace after deconvolution and reflection coefficient function in frequency domain.

As clear from the figure 7, the deconvolved data are not following the reflectivity spectral shape at the frequencies below than 80Hz. So as previously mentioned, we can

apply the color operator to the deconvolved trace right after deconvolution. Three different color operators which explained in the last part are shown in figure 8. It is clear that the third operator is quite different from the two others since it follows from a very different algorithm.

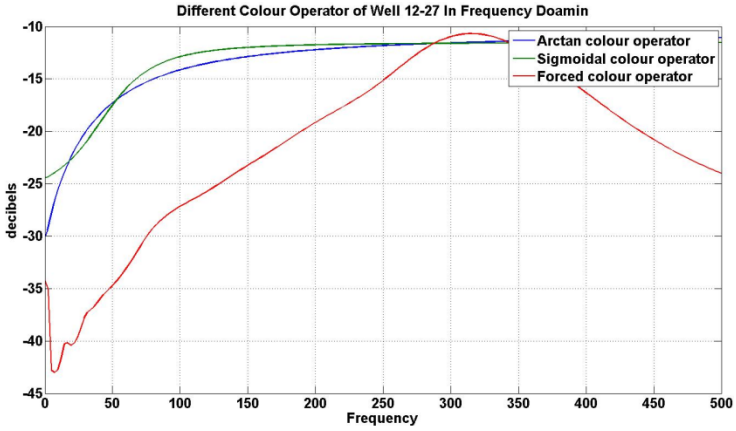

FIG.8. Different color operator derived from reflectivity spectrum of well 12-27.

In the next figures the convolution of these there operators with the deconvolved trace has been shown separately.

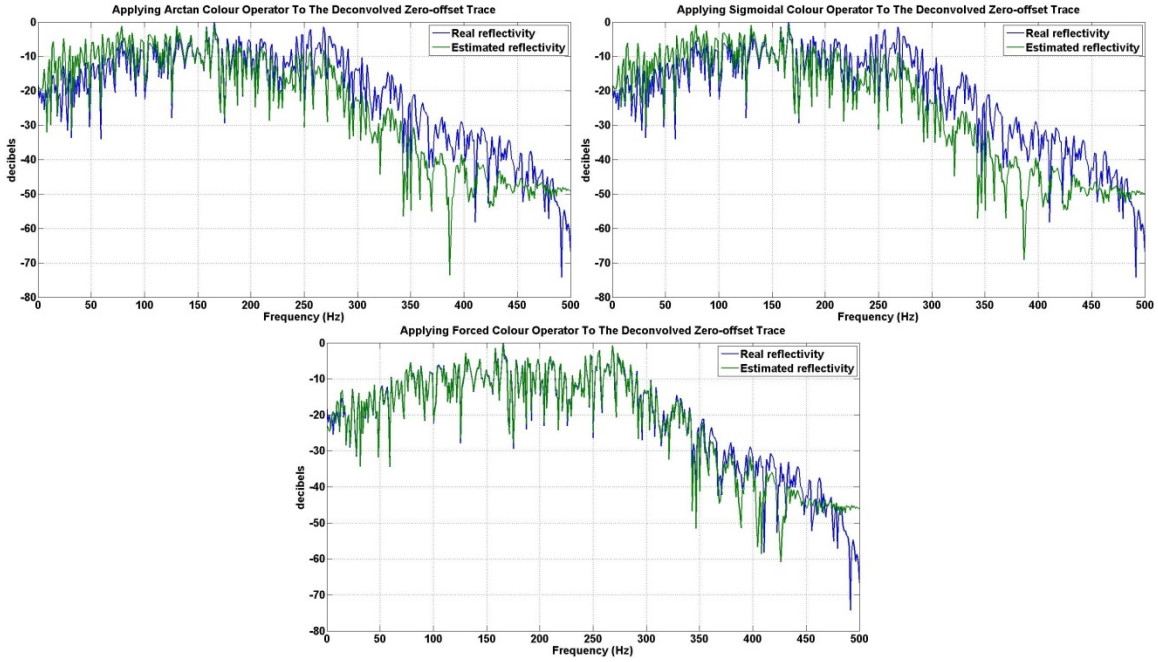

FIG.9. Deconvolved zero-offset synthetic seismic trace after applying (a) Arctan color operator, (b) Sigmoidal color operator and (c) Forced color operator.

Figure 9 shows that the result of last color operator (Forced color operator) has better results than two others. Maximum correlation between well 12-27 reflectivity and final estimated reflectivities are 0.8446, 0.8448 and 0.9835 respectively. In the Forced color operator case, the amplitude spectrum of the deconvolved trace was directly shaped to

conform to that of the reflectivity. But as will be seen in the next part, this operator will become a useful tool for the other non-zero offset traces.

Common source data processing

The general processing flowchart for the common-shot data is given in Figure 10, which can be applied to the synthetic shot gather.

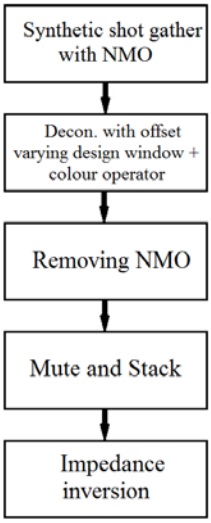

FIG.10. The flowchart of processing common source data.

The synthetic data were created by *Syngram* with 15Hz minimum phase wavelet and log data from well 12-27 located in Hussar. The *Syngram* software assumes the same vertical velocity model for whole studied area. The source was located at the origin and the receivers were located from origin to 1000m with 50m interval. Thus the gather was including 21 traces related to each receiver. Figure 11 shows the velocity model of studied area and the location of source and receivers.

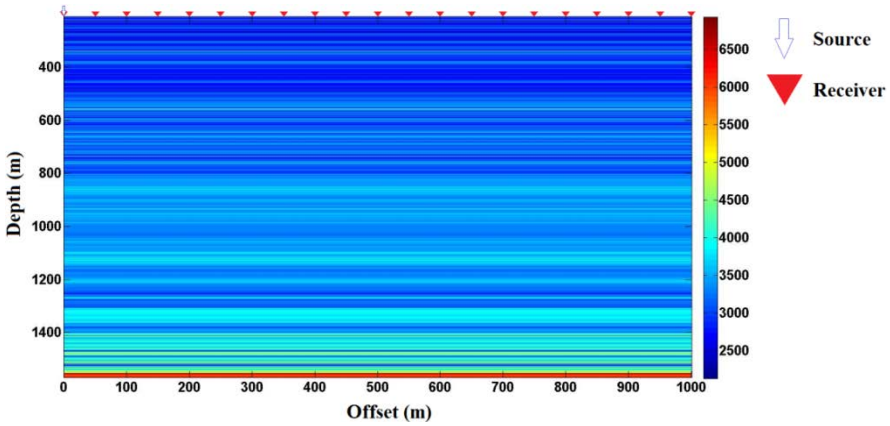

FIG.11. Schematic of source and receivers location for the seismic model.

In figure 12 the noise free synthetic gather from syngram software is shown. The red lines show the design window for deconvolution. The design window for deconvolution

algorithm in the first trace starts from the point at t=0.6 seconds and ends at t=1 second and for the other traces these points are following the RMS velocity trend.

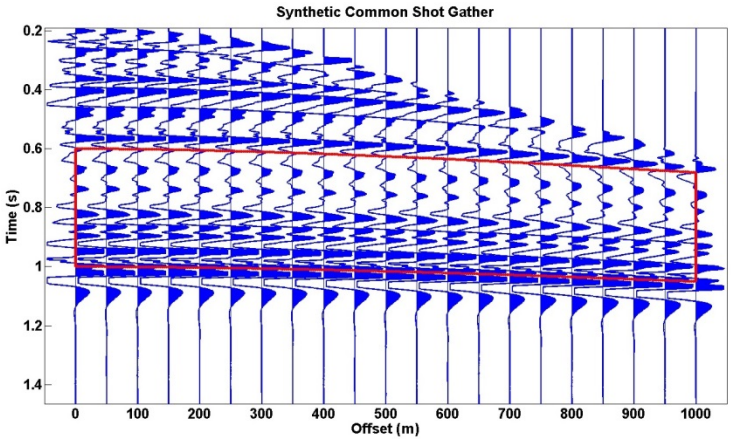

FIG.12. Synthetic common shot gather created by syngram and design window for decon algorithm.

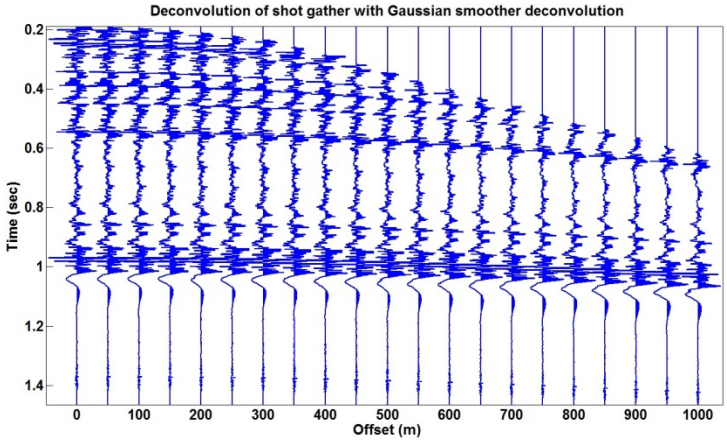

FIG.13. Deconvolution of shot gather with Gaussian smoother algorithm.

The deconvolved traces are including normal moveout which should be removed from them based on RMS velocity. By removing the normal moveout and then stack all the traces, the estimated reflectivity at source location will be obtained.

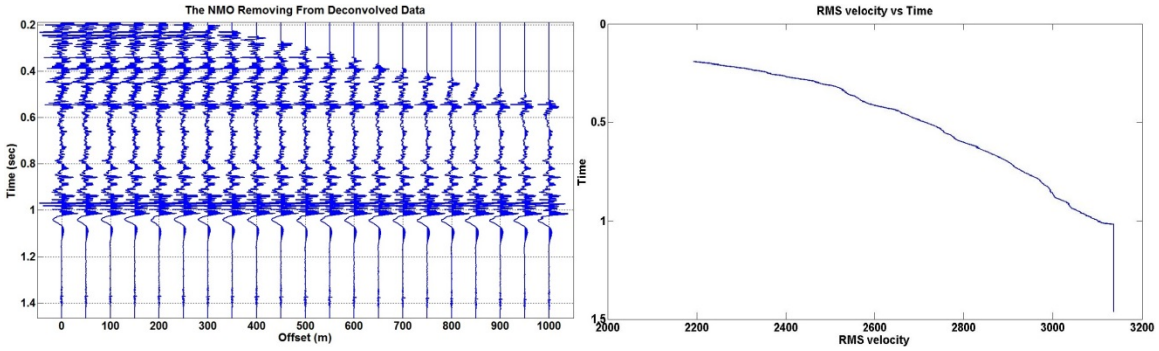

FIG. 14. Deconvolved trace after removing NMO (left) and RMS velocity (right).

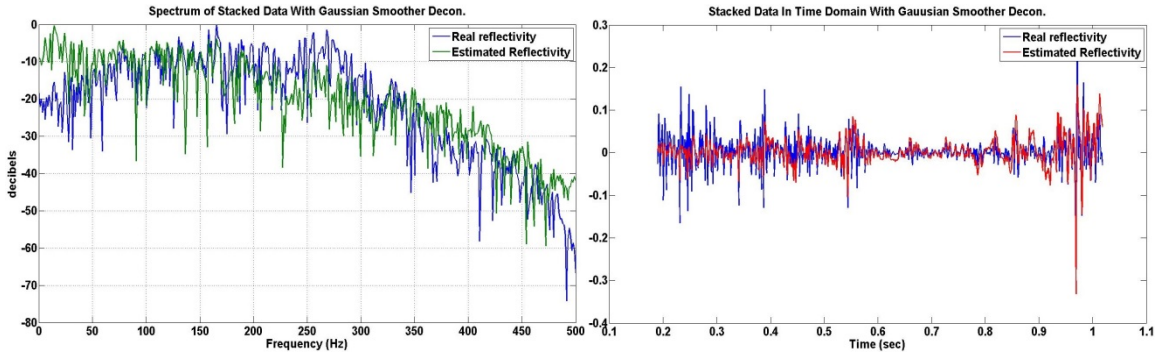

FIG.15. Comparing stacked data and real reflectivity on both frequency and time domain resulted from constant Gaussian smoother decon algorithm.

Even if we use the best smoother in the deconvolution algorithm there are still too many differences in amplitude spectrum in frequencies below than 50Hz. This is the reason that we recommend to use the color operator. If one of the designed color operators applied right after deconvolution to all of the deconvolved traces, the differences on low frequencies will be significant. In figures 16 to 18 the same procedure has been used with the three color operators correction.

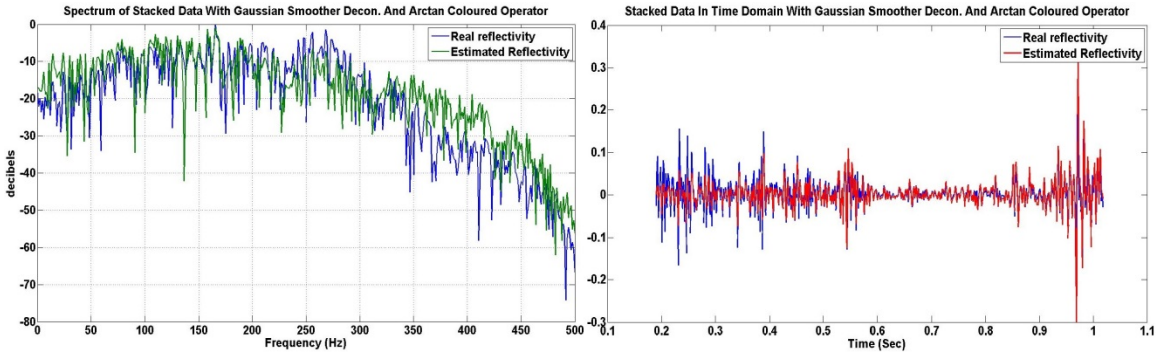

FIG.16. Comparing stacked data and real reflectivity on both frequency and time domain resulted from constant Gaussian smoother decon algorithm after applying Arctan colored operator.

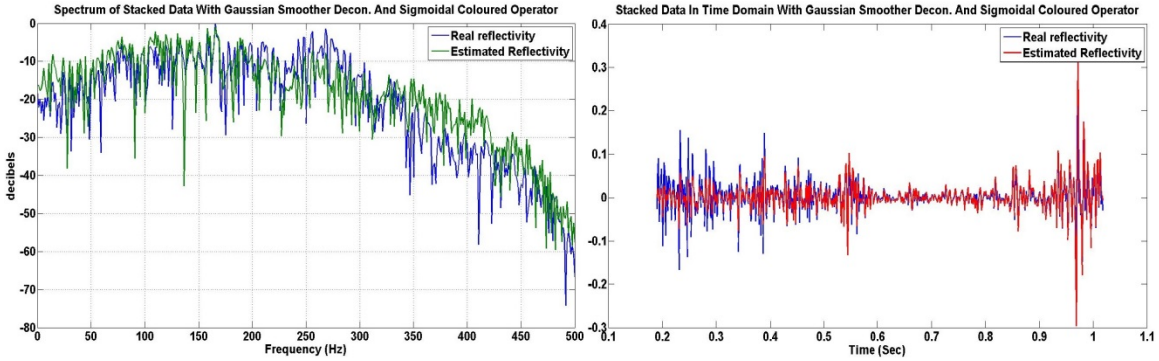

FIG.17. Comparing stacked data and real reflectivity on both frequency and time domain resulted from constant Gaussian smoother decon algorithm after applying Sigmoidal colored operator.

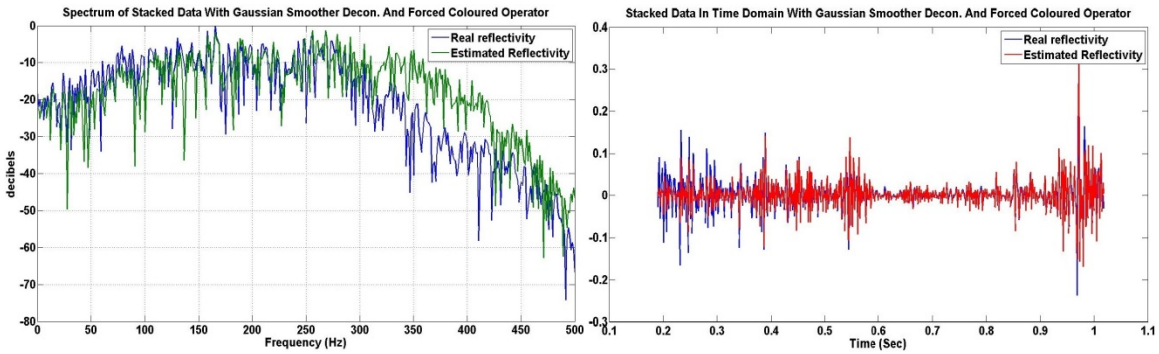

FIG.18. Comparing stacked data and real reflectivity on both frequency and time domain resulted from constant Gaussian smoother decon algorithm after applying Forced colored operator.

ERROR ESTIMATION BY IMPEDANCE INVERSION

Comparing all the results together can give us better idea about the performance of color operator. Especially in frequency domain we need to know which one of our color operators did well in low frequencies. In figure 19 the error function between estimated reflectivity and well reflectivity in time and frequency domain for three different color operators are shown.

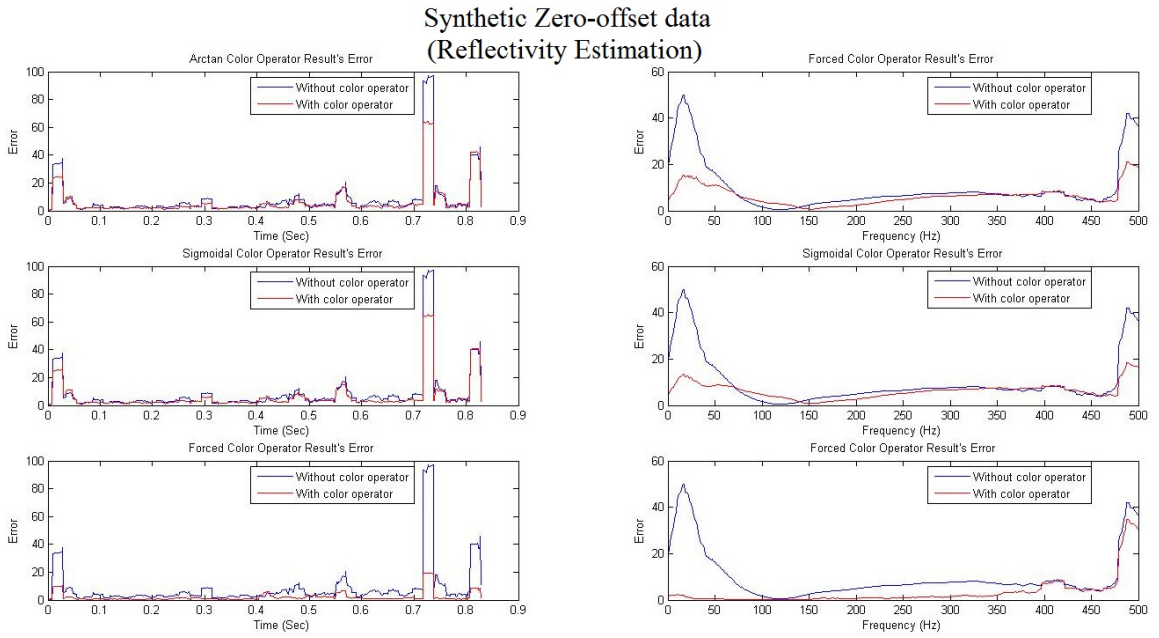

FIG.19. The effect of color operator on estimated reflectivity from synthetic zero-offset data.

The results in time domain shows that using the color operator can improve the estimated data. In frequency domain we are more interested in the region between 0-75Hz which all three color operator did well. Also the results in both time and frequency domain demonstrate that the Forced color operator has better results which we expected that (Figure 20). The result of Forced color operator is significant comparing with the other two operators result.

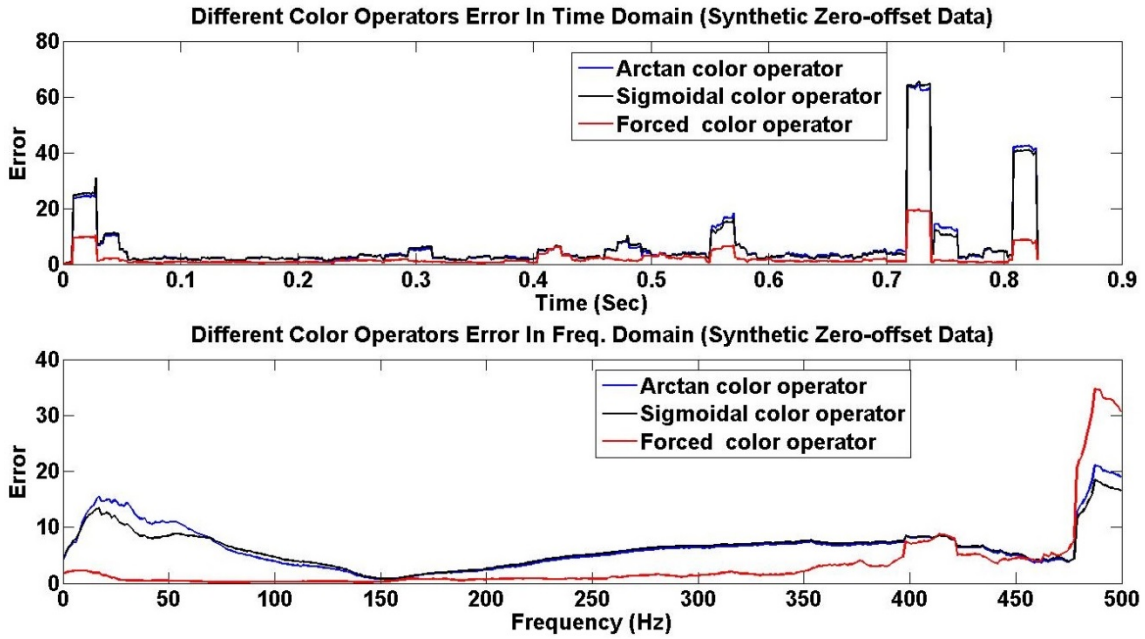

FIG. 20. Comparing three different color operator result's error for zero-offset data in time and frequency domain.

The same comparison can be done for the results of common shot gather data (Figure 21). As shown in this figure, no matter which color operators have been chosen, the estimated reflectivity components are improved in frequencies below than 75Hz after applying them.

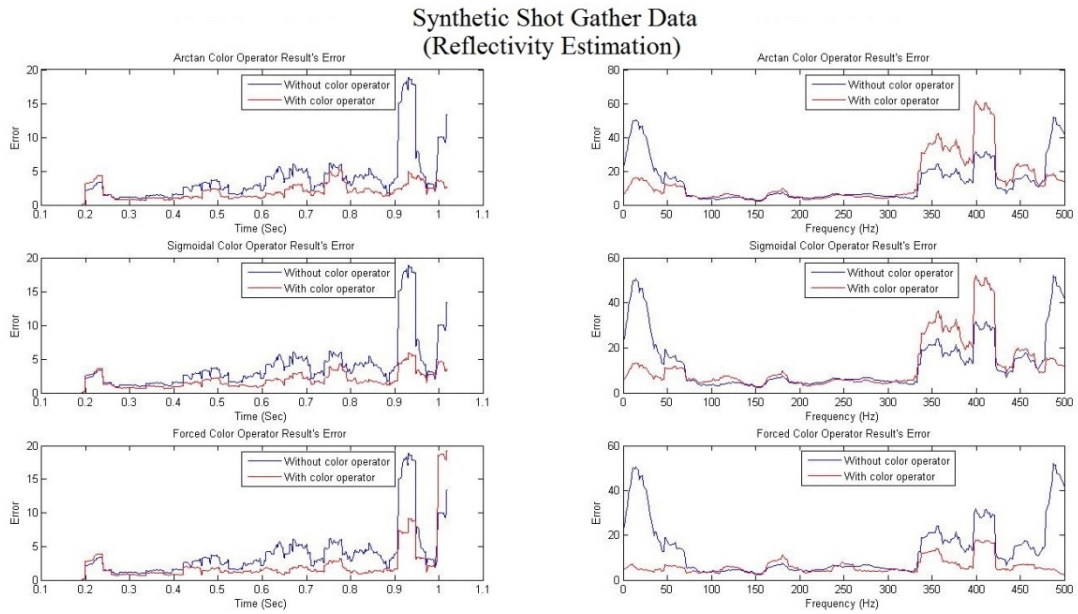

FIG.21. The effect of color operator on estimated reflectivity from synthetic common shot gather.

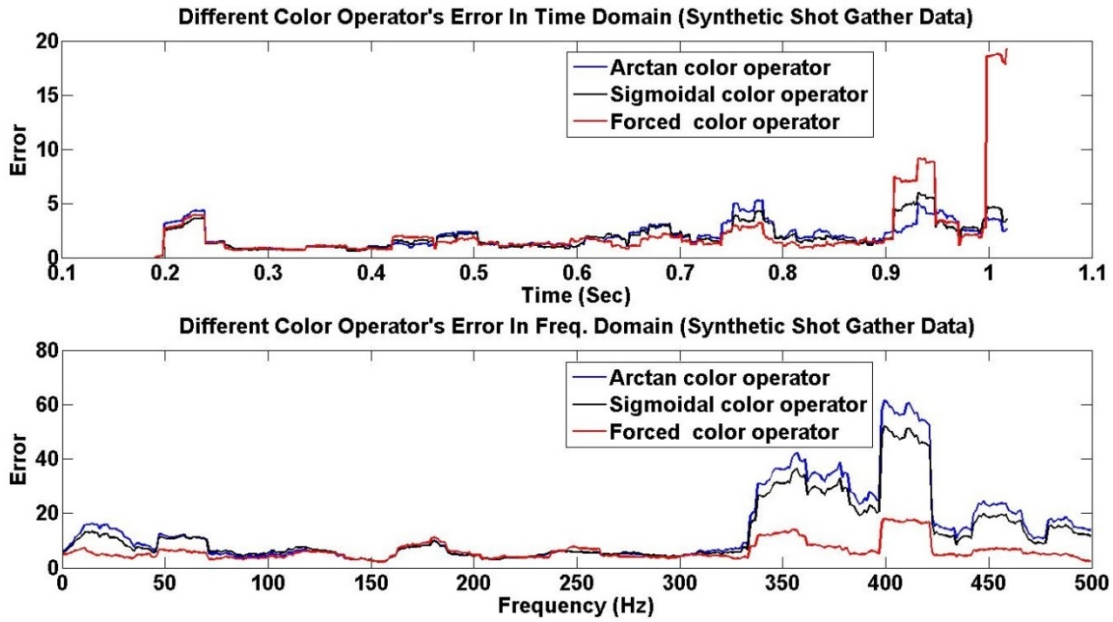

FIG.22. Comparing three different color operator result's error for shot gather data in time and frequency domain.

We can also compute the acoustic impedance of earth to see how color operator can affect the impedance inversion. Acoustic impedance, which is the multiplication of velocity and density, is the rock property. It is possible to show that the acoustic impedance can be computed from the reflectivity via equation 6 (Esmaeili and Margrave, 2013)

$$I_{n+1} = I_1 \prod_{j=1}^{n} \left(e^{2r_j} \right) = I_1 e^{2\sum_{j=1}^{n} r_j}, \qquad (6)$$

where r_j is the reflectivity and I_{n+1} is the acoustic impedance. Thus we can put any of the estimated reflectivities calculated in the last section into the equation 6 and compute the acoustic impedance. The only problem of equation 6 is that this equation is perfect for broadband reflectivities. But any lack of frequencies or misestimation in frequencies leads to the wrong impedance inversion. From the result of reflectivity estimation in the last section it is clear that the amplitude spectrum of estimated reflectivity is not exactly the same as well reflectivity amplitude spectrum. Therefore we expect there should be problem with using equation 6.

For solving this problem Ferguson and Margrave (1996) suggested new algorithm to invert acoustic impedance. Their algorithm is called BLIMP (BandLimited IMPedance) and it is based on recovering the missed frequencies from well log data. There is low and high cut-off frequency in this algorithm which is removing the signal out of this area and then the algorithm import the data from log for these cut-off areas. The next figures are showing the result of impedance inversion of three different color operator's results using BLIMP algorithm for synthetic zero-offset and shot gather data and their errors comparison. The lowest and highest frequencies for the cut-off frequency are 1Hz and

300Hz. This much of low frequency cut-off can help us to see the effect of color operators at low frequency data.

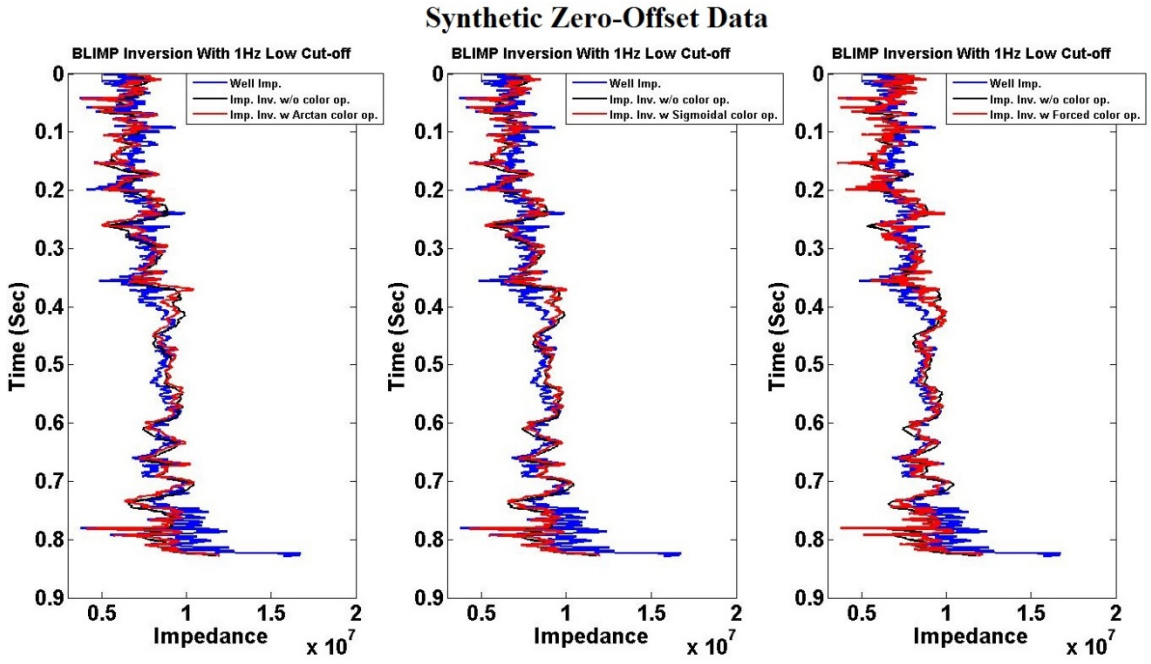

FIG.23. The result of Impedance inversion with BLIMP for different color operator (The low cut-off frequency is 1Hz).

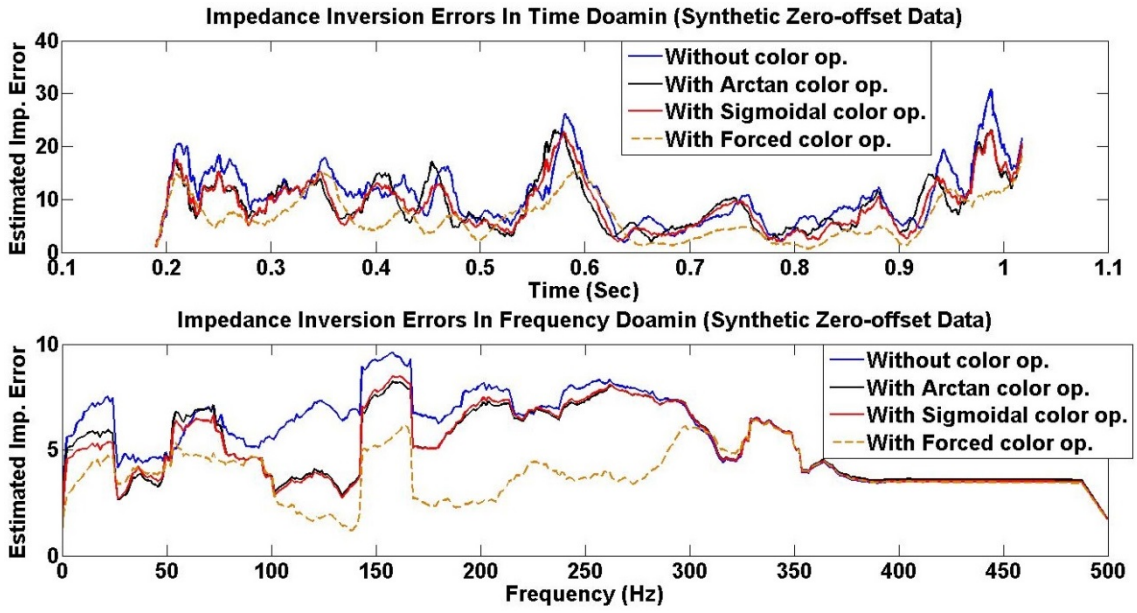

FIG.24. Effect of color operator on impedance estimation errors in time and frequency domain (synthetic zero-offset data).

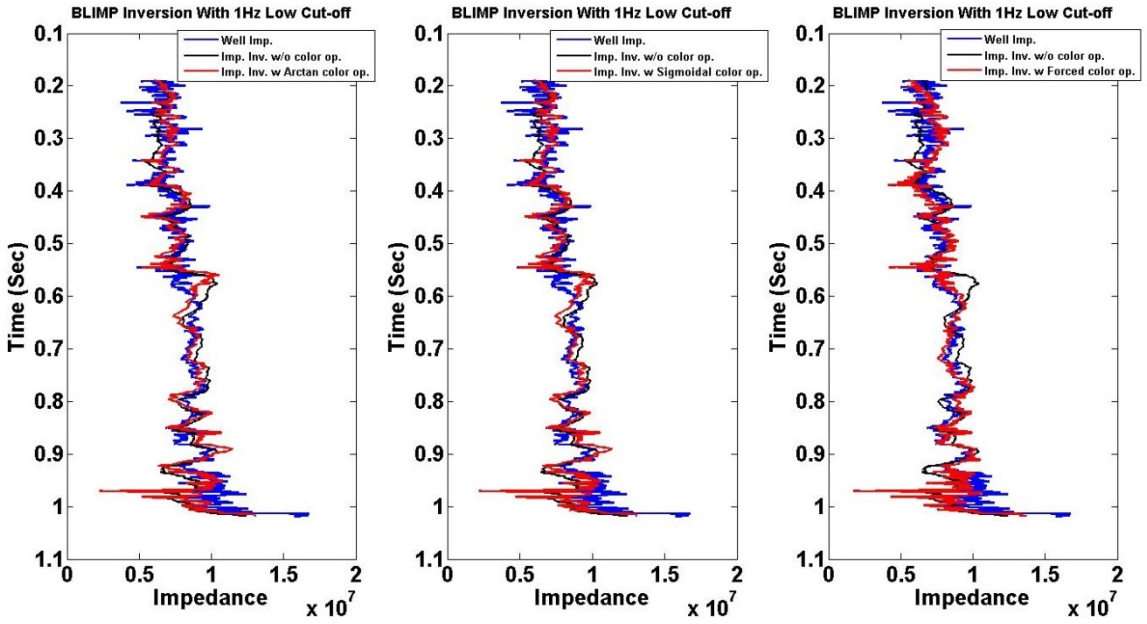

FIG.25. The result of Impedance inversion with BLIMP for different color operator (The low cut-off frequency is 1Hz).

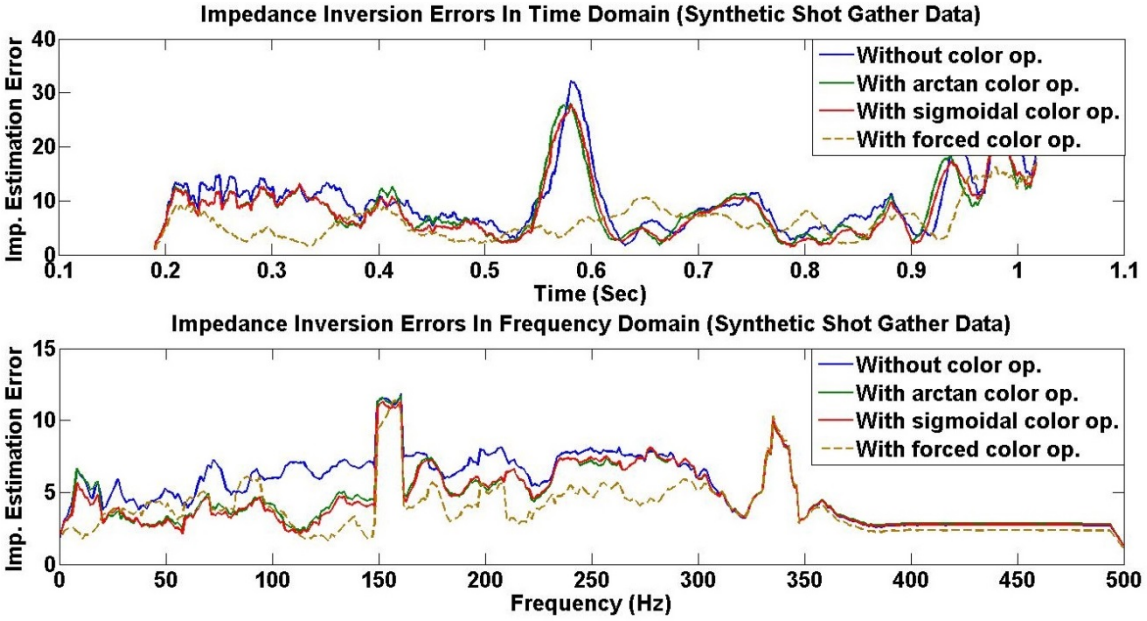

FIG.26. Effect of color operator on impedance estimation errors in time and frequency domain (synthetic shot gather data).

From figure 26, in frequency domain all the results in frequencies below than 2 or 3 Hz are quite the same. This is because of using BLIMP algorithm with the same low frequency cut-off for all resulted reflectivity. But for frequencies higher than this as it is shown, the best choice in low frequency component is Forced color operator. However because of the procedure of deriving Forced color operator, we are not quite sure about the performance of this color operator in other type of data sets. The result of sigmoidal

color operator, because it contains a flattened area in the frequencies below than 20Hz (Figure 5), is clearly better than Arctan color operator. But after 25Hz their results are quite the same since their spectral shape was the same.

CONCLUSION

Conventional deconvolution shapes the spectra to a white one while the real reflectivity always has color spectrum. As was shown, the color operator was designed in different ways from earth reflectivity and when applied after deconvolution to the deconvolved traces, the result of reflectivity estimation was significantly improved. Also, the errors of computed acoustic impedance can be reduced if the color operator applied to the result of deconvolved data.

ACKNOWLEDGEMENTS

We thank the sponsors of CREWES for their supporting and gratefully acknowledge support from NSERC (Natural Science and Engineering Research Council of Canada) through the grant CRDPJ 379744-08. And also we would like to thank all the students and staff in CREWES.

REFERENCES

Esmaeili, S., & Margrave, G. F. (2013). Recovering low frequencies for impedance inversion by frequency domain deconvolution. *CREWES research report, Vol. 25*.

Esmaeili, S., & Margrave, G. F. (2014). Improving frequency domain deconvolution at low frequencies . *CREWES research report, Vol. 26*.

Ferguson, R. J., & Margrave, G. F. (1996). A simple algorithm for bandlimited impedance inversion. *CREWES research report, Vol. 8, No. 21*.

Margrave, G. F. (2002). *Methods of seismic data processing.* Calgary: Department of Geoscience, University of Calgary.

Walden, A. T., & Hosken, J. W. (1985). An investigation of the spectral properties of primary reflection coefficients. *Geophysical Prospecting, 33*, 400–435.